Tellus (1978), *30*, 524–536

Energy transfer in the tropical subcloud layer measured with DC-6 aircraft during GATE

By HERBERT RIEHL and GARY GREENHUT,[1] *National Center for Atmospheric Research,*[2] *P.O. Box 3000, Boulder, Colorado 80307, USA*

and

BRADFORD R. BEAN, *National Oceanic and Atmospheric Administration*

(Manuscript received November 23, 1977; in final form June 13, 1978)

ABSTRACT

Turbulent fluxes of heat and moisture measured during the GARP Tropical Atlantic Experiment of 1974 (GATE) are analyzed with respect to magnitude, distribution with height, intercorrelation and relation to synoptic weather systems. Sensible heat transport on the average is small, whereas latent heat transport is large and nearly always directed upward. In and near convective cloud masses both fluxes become very large compared to clear air, especially sensible heat transfer. A qualitative model of cold and warm downdrafts is presented. There are not only warm, moist updrafts, but also warm, dry downdrafts sinking against buoyancy so that sensible heat fluxes up and down nearly cancel. The role of enhanced fluxes in the general circulation is discussed.

1. Introduction

The tropical oceans are well known to be the major source of thermodynamic energy and angular momentum for the atmosphere. Over the years, various models have been proposed for the transports from the surface to upper layers of the atmosphere. Development of *gust probes* permitting measurement of the rapidly fluctuating air vertical velocity plus improvements in sensors for measuring horizontal wind, temperature and humidity have made it possible to determine fluxes directly from various platforms, including aircraft. The turbulent part of the fluxes which is measured by the new instrumentation, is given by

$$F_s = \overline{(\rho w)' (c_p T)'} \tag{1}$$

$$F_l = L\overline{\rho_v' w'}, \tag{2}$$

where F_s and F_l are sensible and latent heat transfers, the bar denotes the average over a suitably chosen aircraft time interval and the primes are deviations from the time mean. Further c_p denotes specific heat of air at constant pressure, ρ air density assumed constant, T temperature, w air vertical motion, L latent heat of evaporation, and ρ_v density of water vapor.

F_s is not represented by $\overline{(\rho w)' (c_p T_v)'}$, where T_v is virtual temperature. This is a density flux, related to buoyancy of air as emphasized by Brook (1978). On the other hand, Brook points out that past calculations of F_s have ignored the fact that c_{pv}, the specific heat of water vapor, is 1.83 times c_{pd}, the specific heat of dry air. More heat is required to raise the temperature of water vapor by, say, 1 °C than to raise the temperature of dry air. Following his development, similar to that for virtual temperature,

$$c_p = c_{pd}(1 + (c_{pv}/c_{pd} - 1)\,\rho_v/\rho = c_{pd}(1 + 0.83q), \tag{3}$$

where q is specific humidity. Then

$$c_p T = c_{pd}(1 + 0.83q)\,T \equiv c_{pd} T_c \tag{4}$$

and

$$F_s = \bar{\rho} c_{pd}(\overline{w' T'} + 0.83\overline{w' q'}\,\bar{T})$$

[1] Permanent address: Department of Physics, Seton Hall University, South Orange, New Jersey 07079.

[2] The National Center for Atmospheric Research is sponsored by the National Science Foundation.

omitting two small terms. Introducing eq. 2

$$F_s = \bar{\rho} c_{pd} \overline{w' T'} + 0.83 c_{pd}/L \bar{T} F_l. \quad (5)$$

For $\bar{T} = 300\,°K$ near the surface in the tropics, the constant in the second term is almost exactly 0.1, so that

$$F_s = c_{pd} \overline{w' T'} + 0.1 F_l. \quad (6)$$

At large Bowen ratios F_s/F_l the new formulation changes little. Small ratios, however, are typical for most of the tropical oceans because the correlation term $\overline{w' T'}$ is very small. The second term then becomes dominant and can easily reverse the sign of F_s in the subcloud layer before the gradient of potential temperature becomes large near cloud base.

During the Atlantic Trade Experiment of the Global Atmospheric Research Program (GATE), three aircraft equipped with gust probes measured vertical turbulent fluxes. One set of results obtained with a DC-6 aircraft of the National Oceanic and Atmospheric Administration (NOAA) has been published by Bean et al. (1976). The purpose of this report is to present additional analyses of the DC-6 measurements.

2. Data selection and stratification

The DC-6 conducted 30 missions with the gust probe between June and September 1974 off the West African coast, usually in or close to the central (B) ship network of GATE (Kuettner et al. 1974, 1976) in conjunction with other aircraft following a pre-arranged flight plan. From the 30 missions, 440 samples comprising 3300 min of flight time could be processed successfully. In this paper, mostly the flights inside the subcloud layer (below 400-m height) are analyzed. Rain falling on the instrumentation is considered to render certain results doubtful by Bean et al. (1976), especially moisture flux. Since cloud processes are known to have gross effects on turbulence and vertical transports, a distinction was made from the beginning between "clear" samples when the aircraft was not at all or only briefly near heavy cloud areas, and convective samples when the aircraft explored heavy cloud masses found on occasion in the equatorial or intertropical convergence zone active off the west African shore but was not exposed to rain along its track. The GATE International Meteorological Radar Atlas (1977) proved most helpful in locating the aircraft with respect to the mesoscale weather systems.

Bean et al. (1976) have reported in detail on data processing and computational procedures to arrive at the fluxes; they have also made spectral analyses of the fluxes. These subjects are not taken up again in this report; but, Table 1 gives their error estimates of the gust probe data.

Table 2 contains the frequency distribution of sample lengths. Since the aircraft was flying at a rate near 6 km/min, the approximate horizontal distance of each sample class has been included. In principle, the length or duration of samples should be equal for comparability. Often, a sample time of 10 min is used. This would mean a sample distance of 60 km for the DC-6 compared to only 3 km at a fixed surface station for the same time interval if the wind is five m/s. The problem of selecting a sample length truly representative of the processes to be measured is indeed severe. Not only must the mean values of the measured quantities over the sample length be removed but, due to longer trends or large amplitude almost always present in atmospheric data, a linear or even wavy trend must be removed in addition, the latter for instance when computing deviations of daily temperatures from the mean over a year in middle latitudes. Bean et al. (1976) removed the means and linear trends, no doubt the best solution for the present experiment since the "detrending" is not carried so far as to destroy the value of the experiments. However, since the sample sizes ranged from cumulus to cumulonimbus to meso-scale distances, a test on the effect of variability of sample size was made and will be discussed.

Table 1. *Error analysis of gust probe data*

Parameter	Error (RSS)*	Typical value	Units
w'	5.8×10^{-2}	1×10^{-1}	m sec^{-1}
u', v'	1.8×10^{-2}	1	m sec^{-1}
T'	5.0×10^{-2}	1×10^{-1}	°K
ρ'_v	1.07×10^{-2}	5×10^{-1}	g/m^3
T	1.0×10^{-1}	300	°K
ρ_v	2.0×10^{-1}	15	gm/m^3

* RSS = Root sum square.

Table 2. *Frequency distribution of duration and length of legs*

	6–12 1–2	18–36 3–6	42–60 7–10	66–84 11–14	≥90 ≥15	km min	Total legs
Clear	3	59	34	5	7	n	118
Days	3	57	29	4	7	%	
Rainy	1	24	25	9	14	n	73
Days	1	33	36	12	18	%	
Total Cases	4	83	59	14	21		181

3. Ocean temperature relations

In order to relate the measured fluxes to "bulk transport" formulae near the ocean–air interface, ocean temperature (T_o) and the vapor pressure over it must be known. Ocean temperature was monitored continually from the DC-6 with a radiometer in the 10-μm window. Due to variable aircraft height, a correction must be made for absorption of outgoing radiation in the intervening layer. In order to determine correction, all ten days on which the DC-6 flew at several levels were used. The slope of the indicated T_o as a function of height was determined for each day and then all slopes were combined into two classes. As suggested by unpublished radiometer measurements made by one of the authors in the Gulf of Mexico in 1964 in roller-coaster flight patterns, the slope should be smaller in a rain-washed atmosphere than under clear conditions. Therefore, the small sample was subdivided according to mean daily rainfall in the B-network of GATE: less than 10 mm/d, 10 mm/d, and up. This distinction was verified (Fig. 1); a much larger number of cases would, of course, be preferred. The slope on dry days corresponds to a decrease of apparent ocean temperature of 1 °C/50 mb, implying a reduction of black body radiation of 0.01 cal/cm^2 min or 7 W m^{-2}.

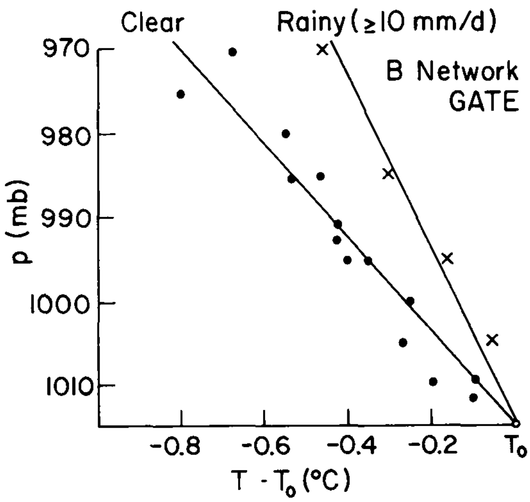

Fig. 1. Reduction of ocean temperature from indicated radiation values at flight level to the ocean surface, for clear and rainy days.

The indicated T_o accordingly was corrected using the slopes of Fig. 1 for each sample. As wind speed increases, ocean surface temperature should decrease because of enhanced mechanical stirring. Such a relation could indeed be found, though with scatter, for the 19 days of DC-6 missions here analyzed (Fig. 2). While clear and rainy days occur at both high and low wind speeds, days with enhanced convection cluster at high speeds. The regression equation is $T_o = 28.2 - 0.07\hat{V}$ (m/s), correlation coefficient $r = -0.40$. If the rainy days with less sunshine are omitted, the same sense of correlation still holds.

4. Average vertical transports of latent and sensible heat

We now turn to a survey of the turbulent energy transfers. Because of the variable duration of samples, all fluxes were first arranged in class intervals according to sample duration and averaged for clear and rainy cases separately. On clear days (Table 3) variation is slight and irregular for F_l as defined by eq. (2). When all observations for these days are summed in two class intervals only, nearly equal transports are obtained showing

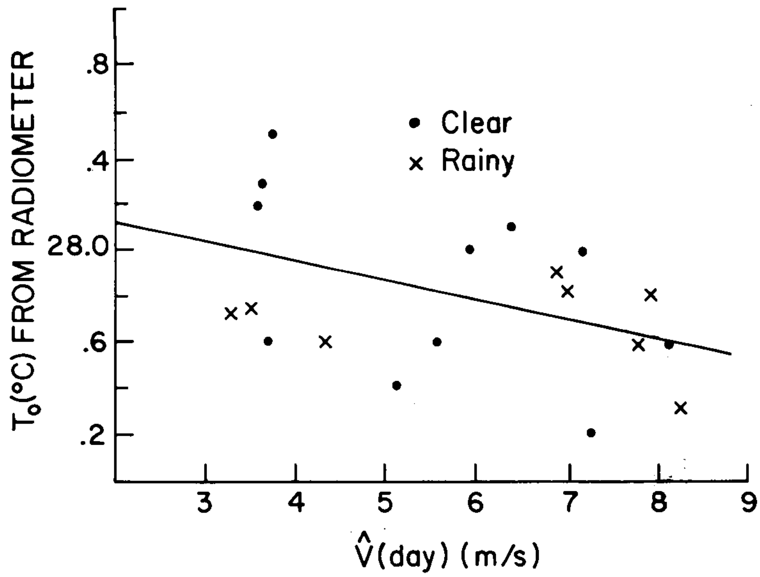

Fig. 2. Correlation between mean wind speed for individual days and ocean temperature corrected using Fig. 1.

Table 3. *Dependence of latent heat transfer on duration of sample*

	Clear legs			Non-rain legs on convective days		
Duration (min)	*n*	F_l/flight W m^{-2}	Two intervals W m^{-2}	*n*	F_l/flight W m^{-2}	Two intervals W m^{-2}
3–6	69	75	82	24	88	94
7–10	34	90		25	100	
11–14	5	70	80	9	17	51
≥15	6	91		13	85	
	114			71		

that longer time or distance oscillations do not contribute to F_l. The result for rainy legs differs surprisingly in the interval 11–15 min from the shorter but also longer legs. Some of the following analyses will be limited to the sample size up to 10 min for rainy days.

The average flux distribution along the vertical (Fig. 3, Table 4) is much smoother for clear than for rainy days averaged according to pressure. F_s, using eq. 6, is largest near the surface and then decreases gradually upward while remaining positive to the highest level flown. When F_s was computed without the correction of eq. 6, there was a crossover point from positive to negative values near 985 mb; thus the correction changes the picture quite dramatically. Convergence of F_s along the straight line drawn in Fig. 3 without the correction for clear days warms the subcloud layer by close to 1 °C/day and, thus, offets half of the net radiation cooling according to Dopplick (1972). On rainy days the heat flux convergence more than balances the radiation deficit.

As usually found, F_l greatly exceeds F_s over the ocean. The corrected curve for F_s lies at about $0.1F_l$ since $\overline{w'T'}$ was very small. Undoubtedly, the small ratio F_s/F_l is related to the fact that potential temperature increases upward above a shallow layer near the ground, whereas specific humidity

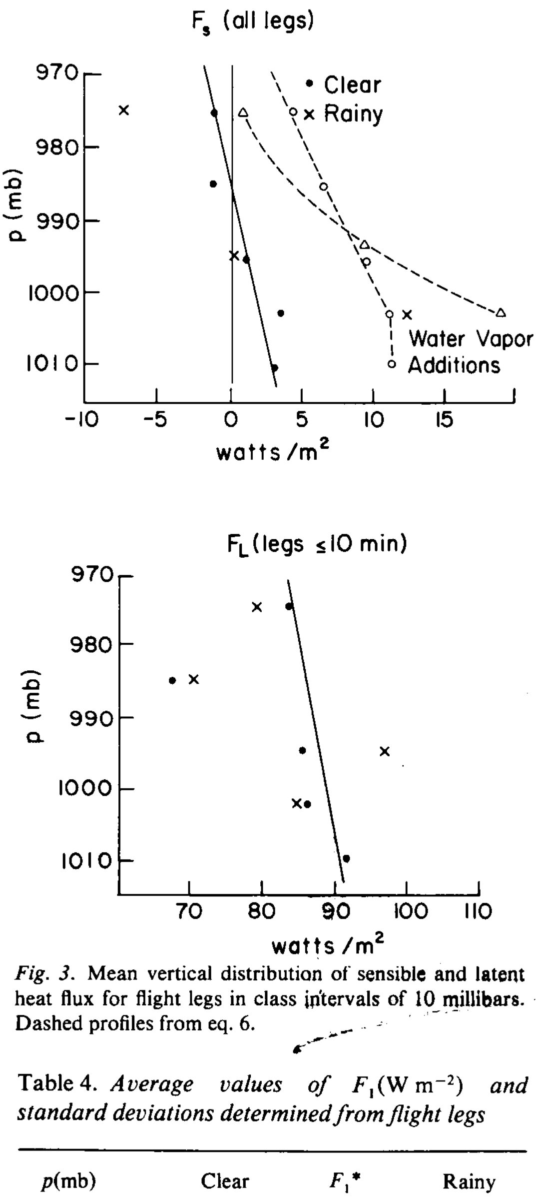

Fig. 3. Mean vertical distribution of sensible and latent heat flux for flight legs in class intervals of 10 millibars. Dashed profiles from eq. 6.

Table 4. *Average values of* F_l(W m^{-2}) *and standard deviations determined from flight legs*

p(mb)	Clear		F_l*	Rainy	
970–980	84	55		78	75
980–990	68	34		70	63
990–1000	82	41		97	83
1000–1005	76	41		75	48
>1005	92	36		no data	

* For flight legs with ≤10 minutes duration only.

and vapor pressure decrease upward all the way in the troposphere limited by saturation vapor pressure. Thus, air temperature readily achieves near-equilibrium with ocean temperature, whereas a large vapor pressure difference is sustained by continuous supply of dry air mixed downward from higher levels. Distribution of F_l along the vertical unexpectedly is far more irregular than that of F_s. Omitting the point in the layer 980–990 mb, where observations were very few, a sloping line can be drawn for clear days; whereas Bean et al. (1976), with equal statistical justification, suggest constant moisture flux in the layer. In that event, however, there would be no accumulation of moisture for export to the continent. The sloping line indicates a moisture convergence of 0.4 g/kg day for the subcloud layer which, in the general setting of GATE, would be reasonable on clear days for accumulation of evaporated water.

More light is thrown on F_l through an examination according to energy transport class intervals (Fig. 4). On clear days all F_l values are positive with strong concentration in the class interval centered on 100 W m^{-2} which corresponds to an ocean evaporation of 0.33 cm/day. For rainy days, the secondary maximum at ≥175 W m^{-2} indicates greatly enhanced evaporation which, in a setting of frequent dry downdrafts, is very reasonable. There are also a few countergradient transports—moist air down—discussed later. Fig. 4 yields a clear portrayal of F_l as affected by convection.

One may ask whether the moisture fluxes of Figs. 3 and 4 can be obtained with a bulk transfer formula if F_l (at least the positive values) approximates Q_e, the latent energy transfer from ocean to atmosphere. Then $F_l \alpha (\bar{q}_o - \bar{q}_a) \bar{V}$, where q denotes specific humidity. Values of $\bar{q}_o$ were obtained from T_o determined earlier; $\bar{q}_a$ was taken as the mean for a flight leg with the mixed layer hypothesis, and $\bar{V}$ was determined in the same way since a systematic wind profile was not observed in the subcloud layer. When summing over all flight legs of an experimental day, a reasonable correlation appears (Fig. 5) which is due mostly to the rainy day's legs. The regression equation is $F_l = 19 + 1.6\hat{V}\Delta\hat{q}$ (units as in Fig. 5; correlation coefficient $r = 0.6$). The correlation is determined mostly by wind speed whereas $\bar{q} - \bar{q}_a$ contributed little.

Individual flight legs were also examined, especially those made below 100-m height yielding the large class interval of 75–125 W m^{-2} on clear days (Fig. 4). There were 17 such legs with 145 min flight time and average sample length of 50

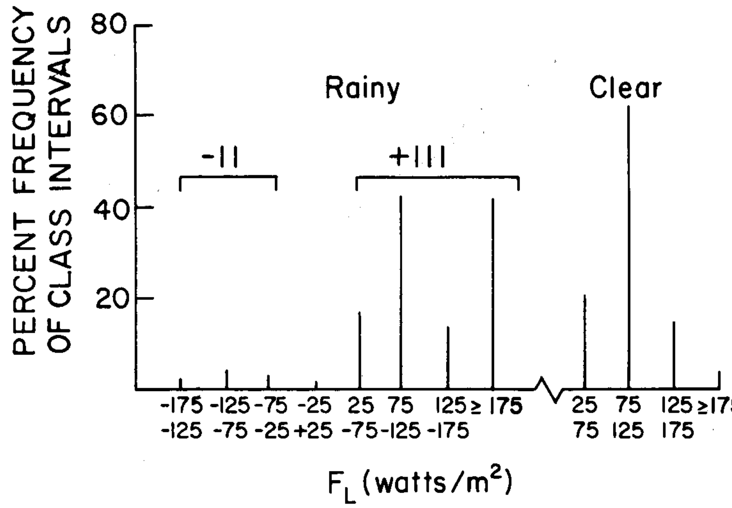

Fig. 4. Percent frequency distribution of class intervals of latent heat transport for clear and rainy days. The negative values are counted separately, and the addition of positive and negative values adds to 100%.

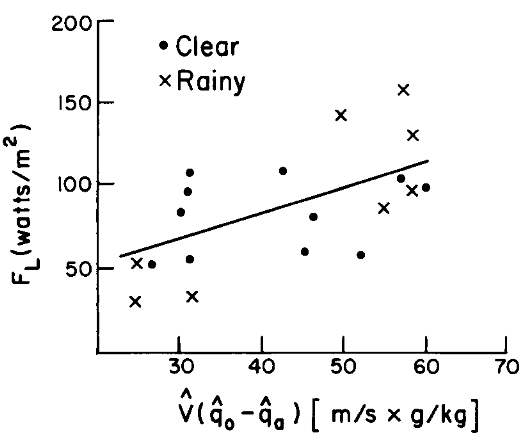

Fig. 5. Correlation between latent heat transport from aircraft data and parameters for bulk formulae computation.

km. Now the product $(\bar{q}_o - \bar{q}_a)\,V$ should be constant; however, $\bar{V}$ varied strongly over the range from three to 11 m/s while $\bar{q}_o - \bar{q}_a$ decreased only very slightly with increasing $\bar{V}$. Assuming the bulk formula is satisfactory for these samples at 10-m height, the mechanism of vertical moisture transport must change drastically already in the lowest 100 m above the ocean.

5. Relations between F_s and F_l. Extreme values

The ratio F_s/F_l is a parameter of great importance in convective turbulence. A positive relation indicates sensible and latent heat transport in the same direction and, if coupled with upward vertical motion, will denote "thermals" of warm, moist air going up, countered by cold, dry downdrafts. Such a relation is pictured in Fig. 6 where w', T', and ρ_v' all have the same sense as far as it is likely to be encountered (point P in Fig. 8). The descent occurs in the middle part of the leg, the ascent at the beginning and end. This leg was flown at the start of a mission on August 10, 1974 in clear air en route from Dakar toward the area of GATE where a heavy cloud mass was moving swiftly westward. The entire mission was executed at 150 meters altitude.

Undilute ascent may well have occurred in the sample of Fig. 6 with $\rho_v' = +0.2$ g/m³ in ascending air at the low altitude. Evidence of thermals extending through a deeper subcloud layer not fully mixed—i.e., with q decreasing upward 2–3 g/kg—can also be found. Such updrafts were encountered, for instance, by a Queen Air of the National Center for Atmospheric Research flying at one-km altitude on August 24, 1972 over the Caribbean Sea just north of the Venezuelan coast

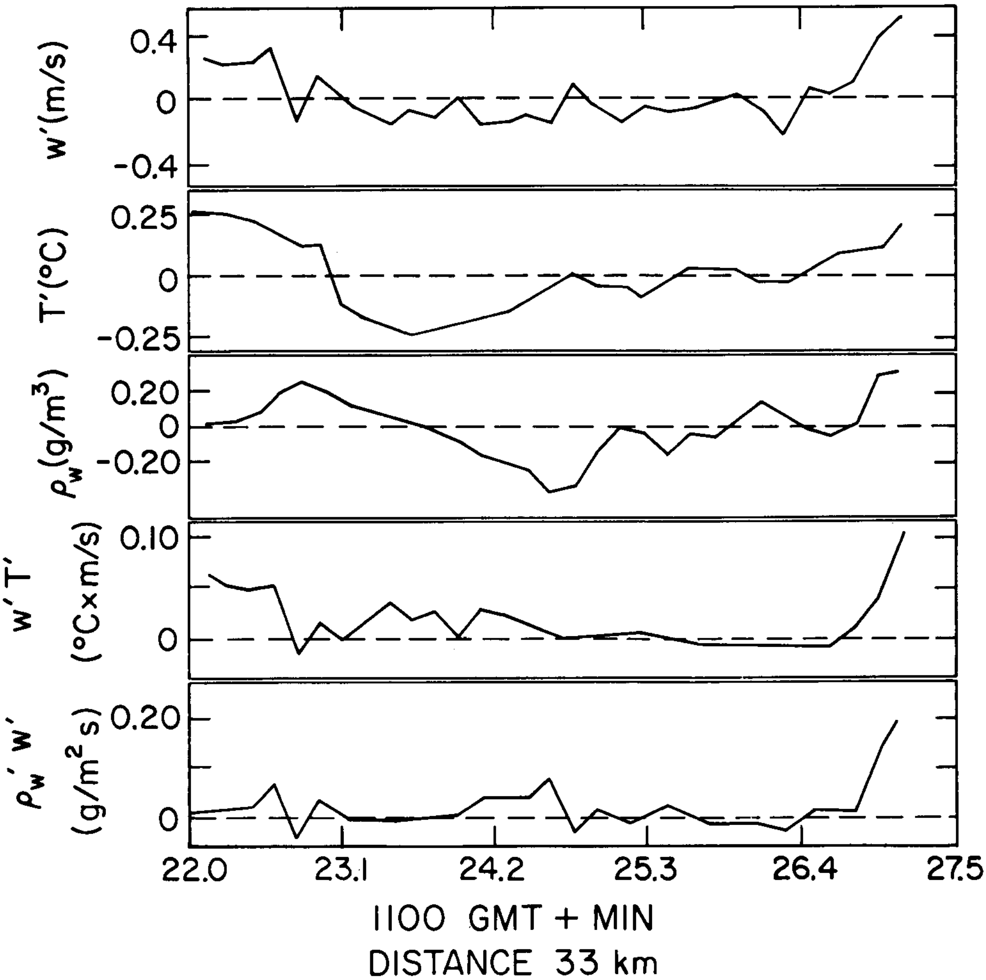

Fig. 6. Turbulent flux data for the first flight leg of the DC-6 aircraft on August 10, 1974, flight altitude 150 meters. The quantities w', T', and ρ_v' are all determined with respect to a zero setting where the mean value over the flight interval and any linear trends from start to finish have been subtracted. The net fluxes of this experiment are entered in Fig. 8 as point P. Note that ρ_w on diagram has same meaning as ρ_V.

(Fig. 7). On coming off the land, the usual regime of intense land turbulence during the day changed to a pattern of quiet flight interrupted by sharp jumps of temperature and dewpoint 1–2 km wide as the airplane just touched small clouds formed near flight altitude. The dewpoint rises to values equivalent to $q = 17$ g/kg which is the surface value, contrasted to clear air values dropping to 12 g/kg.

At the same time temperature drops over 0.5 °C, so that the virtual temperature anomaly is near zero. Either the temperature is cooled by passing through water drops—the well-known wetbulb effect—or the ascents have run out of upward buoyancy.

We see a scatter diagram of F_s and F_l for large transport values in Fig. 8. This is a correlation diagram of correlations with the following meaning in each quadrant:

Upper right:	Warm moist up, cold dry down
Lower right:	Cold moist up, warm dry down
Upper left:	Warm dry up, cold moist down
Lower left:	Warm moist down, cold dry up.

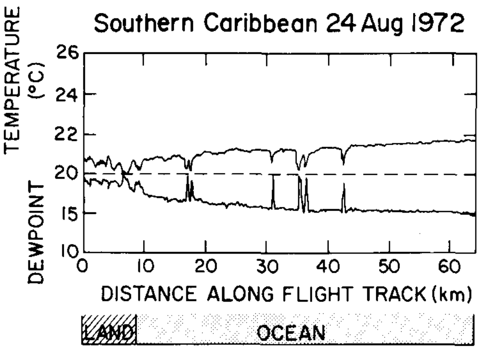

Fig. 7. Trace of temperature and dewpoint recorded by Queen Aire research plane of the National Center for Atmospheric Research flying near 900 mb over the Caribbean just north of Venezuela on August 24, 1972.

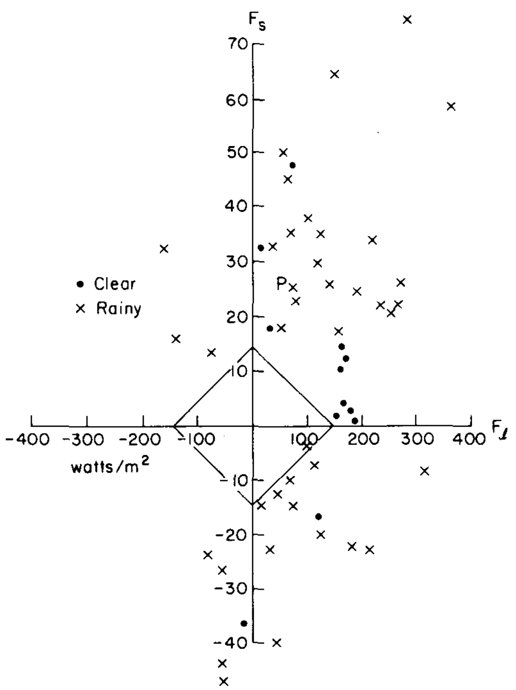

Fig. 8. Scatter diagram of F_s and F_l, all levels combined, for large values only. Point P shows results of experiment in Fig. 6.

The total sample is 52, of which 40 cases are in rainy areas as would be expected. This means that fully 30% of the 181 legs analyzed has $F_s \geq 15$ W m^{-2} and/or $F_l \geq 150$ W m^{-2}. For rainy days the fraction is 55%, more than half.

The diagram is curious in that the left side has very few points. Fully 25% of the cases lie in the quadrant with "sensible heat down—latent heat up." Thus, moisture transport is nearly always upward (85%) along the moisture gradient. But, the upward sensible heat transport in buoyant thermals, at least close to the surface, both from warm, moist ascent and cold, dry descent, is partly cancelled by cool, moist ascent and warm, dry descent. Except for the downdrafts in the late stages of convection (Betts, 1976; Zipser, 1977), the wide prevalence of this mode has not been realized to the authors' best knowledge.

The mechanism may be pictured as shown in Fig. 9. The tephigram depicts an unsaturated downdraft which, at constant relative humidity of 70%, almost exactly reproduces the mean tropical atmosphere over the oceans above 900 millibars (Jordan, 1958). Specific humidity must be increased by evaporation as indicated along the dewpoint curve on the left. If water is available all the way to the surface, the airplane will observe a cold, dry downdraft *in the subcloud layer* arriving at point B (upper right quadrant in Fig. 8). If the supply of water ceases at 900 mb, the downdraft may still reach the surface. But, it will now appear in the lower right quadrant of Fig. 8 as a dry, warm point ending at point C. If the moisture gives out already at 800 mb, the downdraft will not reach the subcloud layer but be stopped at point D. Numerous radiosonde observations show downdrafts with termination between 800 and 900 mb, perhaps more frequently over land than over sea. Fig. 9 also shows a cold and saturated downdraft ending at point A, an event judged rare but nevertheless possible. This wide variety of possibilities is thought to model the distribution of points in the two right-hand quadrants in Fig. 8. It is assumed that downdraft structure is far more variable than updraft structure, which is constrained by the air–sea interaction, and therewith controls the sense of the correlations.

At this point the horizon of flight data examined may be widened to include the rain contaminated legs and samples above the subcloud layer. While the doubtful parts of legs in rain may be recognized readily as spikes in time cross sections (Fig. 12), the samples as a whole appear to convey consistent and believable correlations between w', T', and ρ_v'. All of these samples have been plotted in Fig. 10 which reveals a pattern similar to Fig. 8 but contains much larger numbers, especially for F_s.

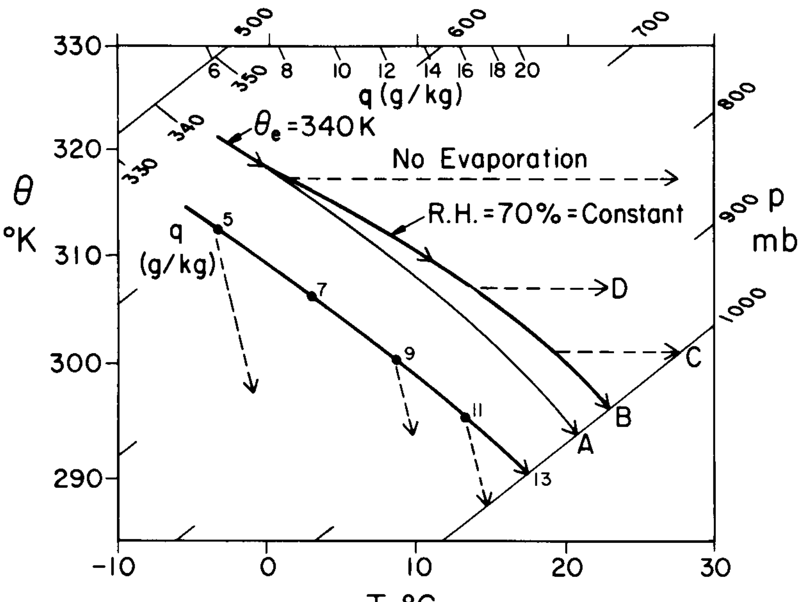

Fig. 9. Tephigram showing temperature and dewpoint curves of downdraft starting at 550 millibars. Numbers along dewpoint curve give successive water increments required for downdraft to continue at 70% relative humidity. End points A–D denote different terminal points dependent on water supply.

The center of buoyant transports, not unreasonably, lies in the cores of radar echoes with deep convection, but so do the warm, dry downdrafts which now comprise 35% of the cases. While the greatly enhanced values of F_s on rainy days arise mainly through the appearance of some very large values they should not be dismissed as erroneous. In convective downdrafts air usually reaches the surface with a temperature around 22 °C, as noted by many observers. Then $T_o - T_a$ rises by an order of magnitude or more compared to clear days, and so should Q_s according to the bulk aerodynamic formula which includes $T_o - T_a$ as one variable.

A total of 60 legs was collected above the subcloud layer, mostly between 1100 and 1500 m. Of these, 26 legs were flown on three clear days, 18 were non-rain legs on two rainy days, and 16 legs were flown in rain on these two days. The scatter diagram (not reproduced) shows similarity with Fig. 10. Of the points, 15 were situated in the upper right, 28 in the lower right, 15 in the upper left and two in the lower left quadrant. The percent frequency in the upper left quadrant is increased with greater distance from the ocean, but we still find the difficult lower left quadrant almost vacant. The lower right quadrant contains almost half of the sample; there are indications also from other aircraft research missions that this mode of energy transfer increases upward and becomes dominant in the middle troposphere. Energy fluctuations there at $p =$ const are almost completely determined by moisture, whereas buoyancy (T_v) has a very high correlation with T. Thus, high energy is transported upward at low T_v; low energy is transported downward at high T_v. This large-scale correlation by frequencies, however, does not take account of the occasional undilute towers with very large upward energy transfer.

For further illustration of the modes of F_s–F_l relations, a sample from a crossing of the main equatorial trough and convergence zone on August 10, 1974 (Fig. 11) has been selected. During approach to the troughline from northwest (Fig. 12), temperature and moisture are out of phase. Vertical motion is positively correlated with moisture and operates against the buoyancy acceleration, yielding point R in Fig. 10. The radar echo was well to the northwest, and convective activity was moving toward west and dying out in the area of the flight at the time of the samples. Thus, the record of Fig. 12 may be related partly to the late stage of convection.

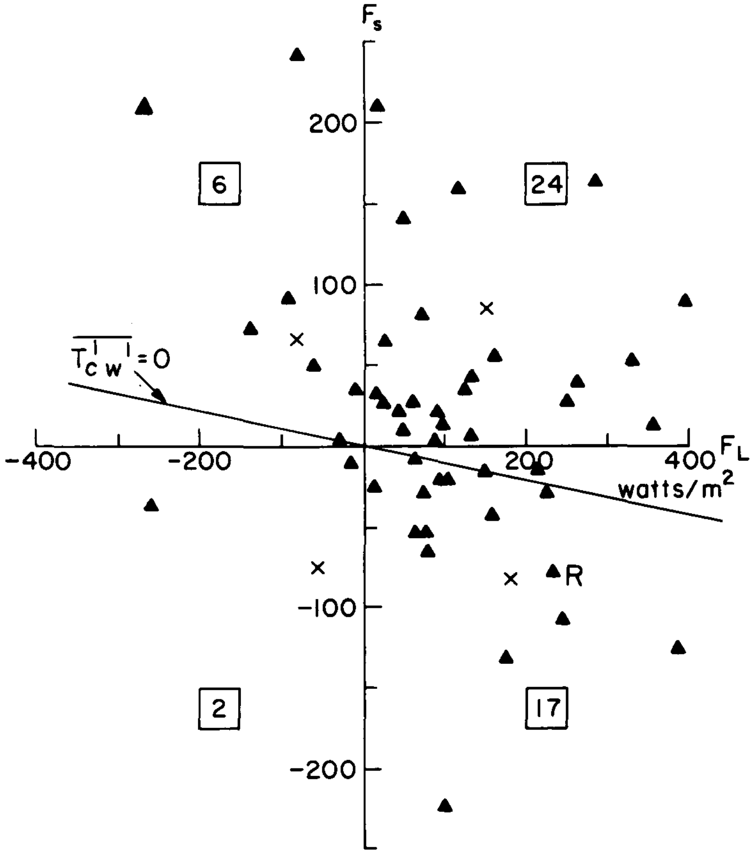

Fig. 10. Same as Fig. 8 for all flight legs near and within radar echoes where rain was occurring (solid triangles). Points marked with crosses are large values that did not fit on Fig. 8. Point R shows the results of the experiment in Fig. 12. The line where $\overline{T_c' w'} = 0$ has also been entered. The difference with the abscissa is very small.

Most energy transfer in Figs. 6 and 12 comes from the mesoscale wavelengths. For instance, in Fig. 12, computation with only five points 11-km distant yields $F_s = -68$ W m^{-2} and $F_l = +200$ W m^{-2}, 90% and better than the values indicated by point R in the illustration. The relation between these fluxes measured over mesoscale distances by aircraft and those determined from ship or stationary ground installations covering, perhaps, $\frac{1}{10}$ of the mesoscale size (cf. Emmitt) remain to be ascertained.

6. The fluxes in relation to the energy balance of the tropics

As indicated especially by Fig. 4, the magnitude of F_l on clear days corresponds very well to climatic values determined for the equatorial trough zone over the oceans with the energy budget and heat transfer methods (Budyko, 1963). The latent heat flux is concentrated near 100 W m^{-2} indicating an evaporation of 125 cm/year in the equatorial zone. The ratio F_s/F_l is positive and small, though above 0.1 with the correction for specific heat of water vapor.

In convective areas F_l is enhanced by a factor of two and F_s, as expected, by a factor of 10–20 indicated in the upper right quadrant in Fig. 10. However, the net value of F_s remains small due to warm downdrafts at negative buoyancy. Irrespective of this new fact, it is of interest to determine the effect of the enhanced fluxes in the upper right quadrants of Figs. 8 and 10 for the energy balance of the equatorial trough zone. Within the convective areas themselves the enhanced F_l, corresponding to evaporation rates of 0.65–1 cm/day,

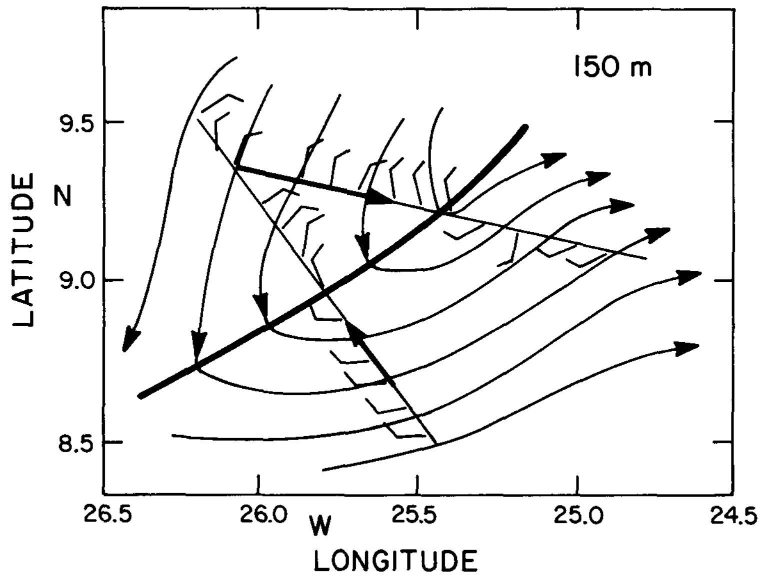

Fig. 11. Winds (knots) and streamlines during double crossing of equatorial trough zone by DC-6 on August 10, 1974 at 150 m height. Cross sections shown in the following figures are marked with heavy arrows.

should play an important role in sustaining convection. In the GATE area the upper 50% of precipitation were produced by ten days, or 19% of all days of the experiment. Average precipitation on these ten days was 1.8 centimeters. Therefore, the evaporation for a day amounts to one-third to one-half of the precipitation and it has the magnitude of moisture advection into the area.

The enhanced fluxes are likely to lead into undilute towers rising to the high troposphere and occupying, roughly, one per-mille of the equatorial area (Riehl and Malkus 1958). This small value, however, only develops above cloud base where the undilute ascents attain maximum upward speed and, therefore, minimum area. In the subcloud layer, where organization takes place gradually, one should expect the updrafts to cover 1% of the total area; this corresponds to the area of mesoscale systems which, of course, are only partly filled with ascending columns. Accepting 1% as a reasonable magnitude and $F_l = 200$ W m^{-2}, the latent heat transport corresponds at most to evaporation of 0.01 cm/day averaged around the globe or 3% of total evaporation. Thus, the towers draw mostly on vapor evaporated over large areas at the "normal" rate and the enhanced evaporation in convective areas contributes almost nothing to the global energy balance, although it is a vital mechanism in bringing the balances about. For an impact on the balance sheet, the enhanced fluxes would have to occur on the synoptic scale of 10% of the equatorial area, which is unlikely, since they are concentrated in the immediate vicinity of active convection only.

7. Conclusion

One of the major results of this investigation is the fact that, whereas, the ratio F_s/F_l is small on the average, about 10% near the surface, it will readily rise to 50% and more in a deep convective cloud system. The large values partly will be positive, partly negative. Positive values correspond to the classical model of buoyant convection carrying energy away from the ocean surface to the higher layers of the subcloud layer and to the cloud layer. The negative values, with contra-buoyant motion on the 10–50 km scale through negative $\overline{w'T'}$ correlation require the formulation of another mechanism for vertical energy transport—all latent heat in this case.

Overall; the turbulent flux measurements verify closely the air–sea latent energy exchange for the area and season given by Budyko's climatic atlas (1963). If a similar result is obtained in some other

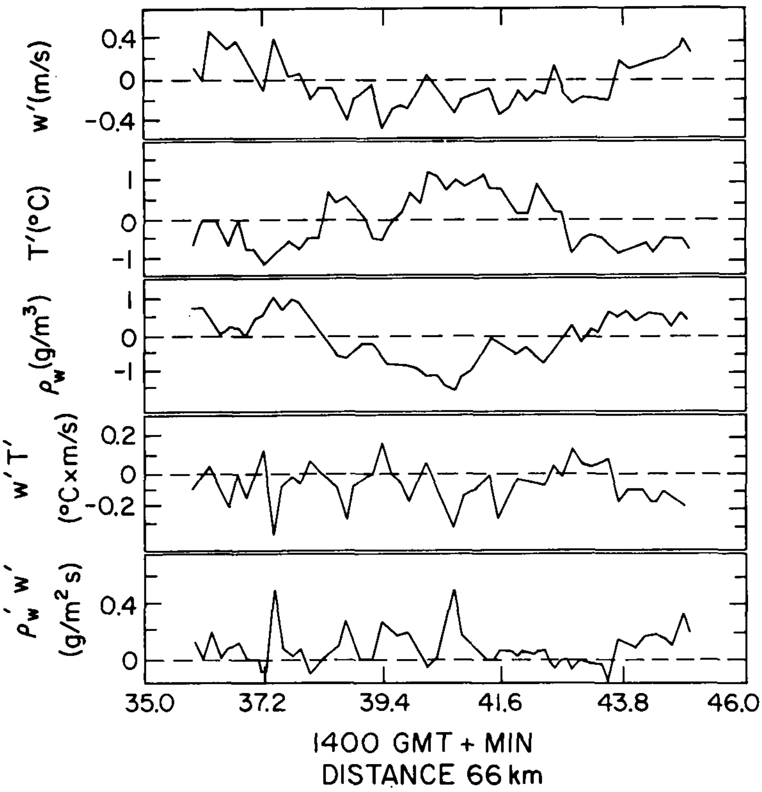

Fig. 12. Turbulent fluxes for approach of DC-6 aircraft to equatorial trough from northwest on August 10, 1974.

areas, the probability will be high that the atlas depicts the energy exchange very well and cannot be subject to gross alteration. Based on satellite measurements, estimates of the tropical energy source have been raised considerably from pre-satellite days and some estimates of long wave radiation have also increased (Dopplick, 1972). Accordingly, it is suggested that a large fraction of the tropical energy surplus must be transported poleward via the ocean currents (Vonder Haar and Oort, 1973). Unless estimates of air–sea exchanges can be raised substantially, however, there appears to be a considerable problem how to remove the additional energy from the ocean.

REFERENCES

Arkell, R. and Hudlow, M. 1977. *GATE International Meteorological Radar Atlas.* Center for Experiment Design and Data Analysis, National Oceanic and Atmospheric Administration. United States Government Printing Office, Washington, D.C. 222 pp.

Bean, B. R., Gilmer, R. O., Hartman, R. F., McGavin, R. E. and Reinking, R. F. 1976. *Airborne measurements of vertical boundary layer fluxes of water vapor, sensible heat and momentum during GATE.* NOAA Tech. Memo ERL WMPO-36, NOAA, Boulder, Colo. 80303, 83 pp.

Betts, A. K. 1976. The thermodynamic transformations of the tropical subcloud layer by precipitation and downdrafts. *J. Atmos. Sci. 33,* 1008–1020.

Brook, R. R. 1978. The influence of water vapor fluctuations on turbulent fluxes. *Boundary Layer Meteorology* (accepted).

Budyko, M. I., ed. 1963. *Atlas of the heat balance of the earth.* Main Geoph. Observatory, Moscow, 69 pp.

Dopplick, T. G. 1972. Radiative heating of the global atmosphere. *J. Atmos. Sci. 29,* 1278–1294.

Emitt, George D. *Tropical cumulus interaction with and* *modification of the subcloud region*, Dept of Environmental Sciences, Univ of Virginia, Charlottesville, Virginia, May 1977, 62 pp.

Jordan, C. L. 1958. Mean Soundings for the West Indies Area. *J. Meteor. 15*, 91–97.

Kuettner, J. P., Parker, D. E., Rodenhuis, D. R., Hoeber, H., Kraus, H. and Philander, S. G. H. 1974. GATE, Final International Plans. *Bull. Am. Meteor. Soc. 55*, 711–744.

Kuettner, J. P. and Parker, D. E. 1976. GATE: Report on the Field Phase. *Bull. Am. Meteor. Soc. 57*, 11–27.

Riehl, H. and Malkus, J. S. 1958. On the heat balance in the equatorial trough zone. *Geophysica*, Helsinki, *6*, 503–538.

Vonder Haar, T. H. and Oort, A. H. 1973. New estimate of annual poleward energy transport by Northern Hemisphere oceans. *J. Phys. Oceanography 3*, 169–172.

Zipser, E. J. 1977. Mesoscale and convective downdrafts as distinct components of squall line structure. *Mon. Wea. Rev. 105*, 1568–1589.

ПЕРЕНОС ЭНЕРГИИ В ПОДОБЛАЧНОМ СЛОЕ В ТРОПИКАХ ПО ИЗМЕРЕНИЯМ С САМОЛЕТА ДС-6 В ТЕЧЕНИЕ АТЭП

Турбулентные потоки тепла и влаги, измеренные в период Атлантического тропического эксперимента ПИГАП в 1974 г. (АТЭП) анализируются по величине, распределению с высотой, взаимной корреляции и связи с синоптическими погодными системами. Турбулентный поток тепла в среднем мал и становится отрицательным выше 990 мб, в то время как турбулентный перенос скрытой теплоты почти всегда направлен вверх. Внутри и вблизи конвективных облачных масс оба потока становятся очень большими по сравнению с таковыми при ясном небе, особенно поток скрытого тепла. Существуют не только поднятия теплого и влажного воздуха, но также и опускания теплого и сухого воздуха, опускающиеся против сил плавучести, так что потоки скрытого тепла вверх и вниз почти уравновешивают друг друга.